Nuclear Magnetic Resonance Imaging of Airways in Humans with Use of Hyperpolarized ^{3}He

Peter Bachert, Lothar R. Schad, Michael Bock, Michael V. Knopp, Michael Ebert, Tino Großmann, Werner Heil, Dirk Hofmann, Reinhard Surkau, Ernst W. Otten

The nuclear spin polarization of noble gases can be enhanced strongly by laser optical pumping followed by electron-nuclear polarization transfer. Direct optical pumping of metastable ^{3}He atoms has been shown to produce enormous polarization on the order of 0.4–0.6. This is about 10^5 times larger than the polarization of water protons at thermal equilibrium used in conventional MRI. We demonstrate that hyperpolarized ^{3}He gas can be applied to nuclear magnetic resonance imaging of organs with air-filled spaces in humans. *In vivo* ^{3}He MR experiments were performed in a whole-body MR scanner with a superconducting magnet ramped down to 0.8 T. Anatomical details of the upper respiratory tract and of the lungs of a volunteer were visualized with the FLASH technique demonstrating the potential of the method for fast imaging of airways in the human body and for pulmonary ventilation studies.

Key words: helium-3; nuclear spin polarization; MRI; pulmonary ventilation.

INTRODUCTION

Magnetic resonance imaging of airways of the human body is difficult with conventional techniques that essentially use the signal of water protons. MRI of lung parenchyma is limited due to short T_2, low signal intensity, and effects of physiological motion and of tissue susceptibility (1).

Established medical imaging procedures in this field involve ionizing radiation. Diagnostic imaging of the lungs is mainly performed by means of x-ray chest films and x-ray computed tomography (CT). Both techniques do not allow direct evaluation of airway ventilation. Up to now, ventilation imaging studies could only be done with use of radioactive gases or ultrasonically generated technetium-99m tagged aerosols. Such nuclear medicine methods, however, lack the spatial resolution and cross-sectional anatomical visualization that are routinely achieved by MRI.

The use of nuclei other than proton (^{1}H) and sodium (^{23}Na) as the source of the MR signal for fast MRI *in vivo* is largely hampered by low gyromagnetic ratio and low abundance. As a consequence of limited sensitivity, spectroscopic imaging using phosphorus (^{31}P) in tissue (2) or fluorine (^{19}F) during fluoropyrimidine chemotherapy (3) requires measurement times on the order of 10 min and detection volumes (voxel) that are $\sim 10^4$–10^5 times larger than those of MRI with tissue water protons.

An enhancement of MR signals of rare nuclei (I) can be achieved by utilizing their coupling to abundant spins (S) with large gyromagnetic ratio. Driving the S spins produces an I-spin state far from thermal polarization given by Boltzmann statistics. For example, selective radiofrequency (RF) irradiation at the Larmor frequency of proton spins amplifies the MR signals of ^{13}C or ^{31}P nuclei owing to dipolar coupling with neighboring protons in liquid phase (nuclear Overhauser effect) (4).

For an ensemble of spin-½ nuclei in an external field, with magnetic induction $\vec{B}_0 = (0,0,B_0)$, spin polarization is defined by

$$p = \frac{N(\uparrow) - N(\downarrow)}{N(\uparrow) + N(\downarrow)}, \qquad [1]$$

where $N(\uparrow)$ is the number of spins with parallel and $N(\downarrow)$ the number of spins with antiparallel orientation with respect to the static field. The MR signal of a given nuclear species is proportional to the product of p and the number of spins in the detection volume. For protons in living tissue, the thermal spin polarization

$$p_B(^1H) = \frac{\mu_I(^1H) \cdot B_0}{k_B \cdot T} \cong 1.0218 \cdot 10^{-3} \frac{B_0/\text{Tesla}}{T/\text{K}} \qquad [2]$$

is $\sim 5 \times 10^{-6}$ in a typical field of $B_0 \cong 1.5$ T and at $T = 310$ K body temperature (μ_I = nuclear magnetic moment, k_B = Boltzmann constant, T = absolute temperature).

An enormous enhancement of the nuclear spin polarization of spin-½ noble gas atoms far above thermal polarization can be produced through transfer of angular momentum mediated by contact interaction $\vec{I} \cdot \vec{S}$ of nuclear spins (spin vector operator $\vec{I}$) and the highly polarized electron spin system ($\vec{S}$) of optically pumped alkali-metal vapor (5). For example, laser-optical pumping and spin exchange with rubidium spins increases the polarization of ^{129}Xe nuclei in a gas (6–8).

A different polarization technique applicable to ^{3}He nuclear spins is based on direct optical pumping of metastable atoms and subsequent metastability exchange scattering (9). Recently, an efficient technique for producing large amounts of polarized ^{3}He samples at a convenient pressure was developed (10–12), which is a prerequisite for application in MRI (13).

MRM 36:192–196 (1996)

From the Forschungsschwerpunkt Radiologische Diagnostik und Therapie, Deutsches Krebsforschungszentrum (DKFZ), Heidelberg (P.B., L.R.S., M.B., M.V.K.); and the Institut für Physik, Johannes Gutenberg-Universität Mainz, Mainz (M.E., T.G., W.H., D.H., R.S., E.W.O.), Germany.

Address correspondence to: Peter Bachert, Ph.D., Forschungsschwerpunkt Radiologische Diagnostik und Therapie, Deutsches Krebsforschungszentrum, Im Neuenheimer Feld 280, 69120 Heidelberg, Germany.

Received February 6, 1996; revised March 26, 1996; accepted April 4, 1996.

This study was supported in part by grants from the Tumorzentrum Heidelberg/Mannheim and the Roland-Ernst-Stiftung.

0740-3194/96 $3.00

The pioneering work on the use of laser-polarized noble gas isotopes for biological magnetic resonance imaging was done by W. Happer and co-workers. They performed MRI of excised lungs of a mouse (14) and of lungs of a guinea pig (15) with hyperpolarized ^{129}Xe and ^{3}He, respectively. The purpose of our study is to establish ^{3}He MRI *in vivo* in humans in a conventional whole-body MR scanner. The ultimate goal is to provide a new modality for studies of pulmonary ventilation.

MATERIALS AND METHODS

Hyperpolarized ^{3}He of high density was produced with a technique developed recently at the University of Mainz. The procedure, which allows generating large quantities of polarized samples, is described elsewhere (10–13). In short, it uses metastability exchange scattering as polarization transfer mechanism from optically pumped metastable ^{3}He atoms to the ground state atoms. Efficient pumping is achieved by means of near-infrared laser light on condition of low pressure discharge for populating the metastable state. A pressure of several bars is achieved by mechanical compression of the optically pumped gas with a specially developed nonmagnetic compression device (10, 11).

The resulting nuclear spin polarization $p(^3\text{He}) \cong 0.6$ is $\sim 10^5$ times larger than the polarization of tissue water protons at thermal equilibrium used in conventional MRI and overcomes easily the loss in MR signal due to the lower density of spins in the gaseous phase. For pure ^{3}He gas, atom-wall interactions dominate T_1 relaxation. Appropriate materials and coating of walls of storage cells result in ^{3}He relaxation times $T_1 > 100$ h (12). A magnetic field of a few Gauss suffices to store the enhanced ^{3}He spin magnetization for many hours. Polarized samples were produced the day before MR measurements took place at Heidelberg, which is located about 100 km from Mainz.

^{3}He MR experiments were performed in a whole-body MR system (MAGNETOM 63/84 SP 4000; Siemens, Erlangen, Germany), which is equipped with a superconducting magnet of variable field strength $B_0 = 0.1$–2.0 T (Helicon; Siemens). ^{31}P RF transmit/receive hardware was used for detection of ^{3}He, which necessitated ramping down the field. Three antenna systems that we use for *in vivo* ^{31}P MR spectroscopy at the standard field strength $B_0 = 1.5$ T of the tomograph were employed at $B_0 = 0.8$ T corresponding to 25.9 MHz Larmor frequency of the ^{3}He spins. Experiments with glass cells were performed with planar surface coils (H.-J. Zabel, DKFZ) of 5 and 7.5 cm ∅, while a crossed Helmholtz resonator (Siemens) with loops of 17 cm ∅ (25.9 MHz) and of 22 cm ∅ (63.6 MHz) was used for *in vivo* ^{3}He MRI of the human neck and thorax. The RF antennas were tuned while loaded with a water sample.

Glass cells filled with highly spin-polarized ^{3}He gas ($p \cong 0.4$, $V = 100$–300 cm^3, pressure 3 bar) were rapidly moved from the transport coil placed at the end of the patient table into magnet center. Macroscopic diffusion motion of polarized atoms through a magnetic field inhomogeneity establishes a relaxation mechanism with rate constant $1/T_1 \propto [\Delta B_0/\Delta z \cdot 1/B_0]^2$ (16). However, the whole-body magnet has the advantage of sufficiently small relative gradients $\Delta B_0/\Delta z \cdot 1/B_0$ of the stray field ($<10^{-2}$/cm as measured at $B_0 = 0.8$ T) to exclude rapid depletion of the polarization when the sample is passing this critical zone.

Because every excitation destroys nonequilibrium polarization that cannot be recovered, small spin flip angles are mandatory. This suggests use of the fast low angle shot (FLASH) (17) imaging technique with weak RF pulses. During all measurements the MR scanner was operated in experimental mode with the automatic transmitter adjustment switched off to avoid the large flip angles applied during this procedure. Sequence parameters of the ^{3}He experiments were set according to previous tests of the antennas.

The half-life of the enhanced ^{3}He spin polarization was determined in an experiment with a sample contained in a glass cell. Sixteen MR spectra were acquired consecutively during a period of 515 s by means of nonselective 1-pulse excitations of ^{3}He nuclei (flip angle $\alpha \cong 1°$, number of averages $N = 1$).

After successful completion of these studies, *in vivo* ^{3}He MRI experiments were performed with a 27-year-old healthy volunteer. Informed consent according to the ethical guidelines of the institutional review board was obtained from the volunteer prior to the MR examinations.

The volunteer was in supine position, his head and neck (Experiment 1) or thorax (Experiment 2) located within the Helmholtz antenna. The glass cell filled with polarized ^{3}He was placed on top of his chest. For the next step we considered that paramagnetic molecular oxygen is probably the dominant source of T_1 relaxation of ^{3}He *in vivo*. Saam *et al.* (18) studied the spin lattice relaxation of ^{3}He in the presence of O_2 and found a linear relationship between $1/T_1$ and the density of O_2 (for a temperature range $T \sim 200$–370 K, $B_0 = 1.41$ T). Accordingly, the volunteer had to first inhale pure ^{4}He gas in two deep-breathing cycles to reduce the concentration of oxygen in the airways as much as possible. Immediately afterward, he took the outlet of the vial, which contained polarized ^{3}He, in his mouth, opened the glass valve, inhaled the ^{3}He gas, and held his breath.

At this point a series of seven consecutive slices in sagittal orientation was acquired with 2D FLASH in a measurement time of 14 s (Experiment 1: repetition time $TR = 98$ ms, echo time $TE = 5$ ms, slice thickness TH = 30 mm, field of view FOV = 250 × 250 mm^2, image matrix 128 × 256, $N = 1$, bandwidth BW = 195 Hz/pixel) or 28 s (Experiment 2: $TR = 98$ ms, $TE = 5$ ms, TH = 30 mm, FOV = 300 × 300 mm^2, matrix 256 × 256, $N = 1$, BW = 195 Hz/pixel). The experiment was performed three times in rapid succession. During the total acquisition periods of 3 × 14 s and 3 × 28 s, respectively, the volunteer was holding his breath, his nose being closed by tape.

To estimate the flip angle α applied in the *in vivo* ^{3}He FLASH MRI experiment, the image signal intensities were measured in a selected region of the images of the ventilated lung. Assuming that the RF excitations are the only cause of signal depletion (neglecting T_1 relaxation and transversal coherences) signals S_1 and S_2 observed in

subsequent experiments are related by $S_2 = S_1 \cdot (\cos\alpha)^n$ where n = number of RF excitations. Hence arccos $(\sqrt[n]{S_2/S_1})$ gives the upper limit for the applied flip angle α.

After ramping the whole-body magnet back to the field strength B_0 = 1.5 T and repositioning the volunteer, ^{1}H 2D FLASH imaging of the same anatomical region was performed with use of the 63.6-MHz loops of the crossed Helmholtz resonator (MRI of head and neck: α = 10°, TR = 98 ms, TE = 5 ms, FOV = 250 × 250 mm^2, matrix 128 × 256, TH = 4 mm, N = 2, BW = 355 Hz/pixel) or with use of the body resonator (MRI of thorax: α = 10°, TR = 6.5 ms, TE = 3 ms, FOV = 300 × 300 mm^2, matrix 128 × 128, TH = 10 mm, N = 1, BW = 355 Hz/pixel).

RESULTS

Following 1-pulse excitations with small flip angle (≅1°), free induction decays were obtained with good signal-to-noise ratio (SNR) from polarized ^{3}He samples contained in glass cells. The optimum was SNR ≅ 2400:1 in experiments with the 7.5 cm ∅ surface coil. Optimization of magnetic field homogeneity (shim) was not necessary (minimum linewidth $\Delta\nu_{1/2}(^3\text{He}) \cong 1.2$ ppm in these experiments, corresponding to $T_2^* \cong 10$ ms).

In a series of 1-pulse excitations of ^{3}He nuclei in a glass cell, we observed a slow decay (half-life T_1 ~280 s) of the enhanced ^{3}He spin magnetization toward its thermal equilibrium value (Fig. 1). Since weak pulses were employed, the signal decay results from spin-lattice relaxation and is not induced by RF irradiation. Because of longevity of the enhanced polarization, several series of 3D and multislice 2D ^{3}He FLASH imaging of glass cells were possible with in-plane spatial resolution on the order of 1 × 1 mm^2. Figure 2 shows ^{3}He FLASH images of various glass cells filled with polarized gas.

Our first *in vivo* ^{3}He images were obtained from the upper respiratory tract of the volunteer after inhalation of hyperpolarized ^{3}He gas (Experiment 1). Figure 3a shows the results of the ^{1}H FLASH examinations of this anatomical region performed at B_0 = 1.5 T with use of the 63.6-MHz loops of the crossed Helmholtz resonator. Figures 3b and 3c show *in vivo* ^{3}He FLASH images acquired at B_0 = 0.8 T during the first series (Fig. 3c with inverted gray scale).

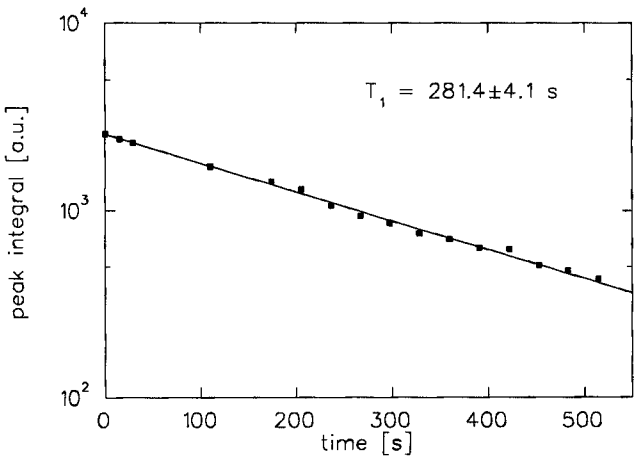

FIG. 1. Decay of enhanced spin polarization of ^{3}He nuclei contained in a glass cell (B_0 = 0.8 T). Peak areas obtained from ^{3}He MR spectra acquired with 1-pulse excitations are plotted as a function of time.

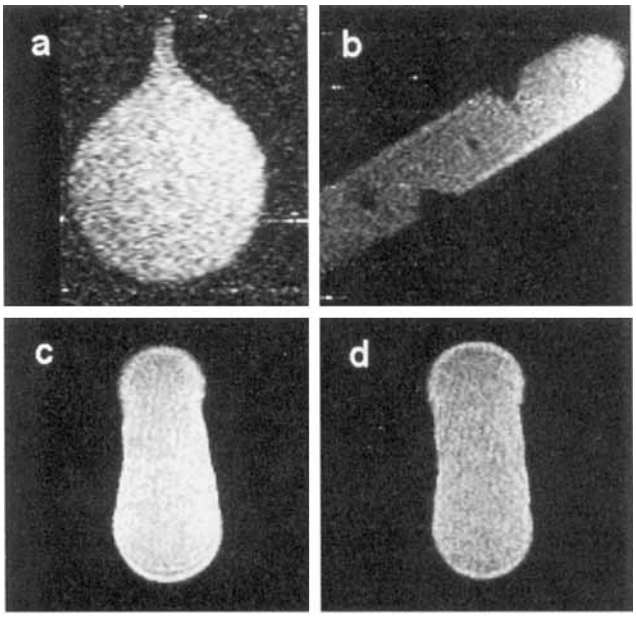

FIG. 2. ^{3}He FLASH MR imaging at B_0 = 0.8 T (25.9 MHz Larmor frequency) of various glass cells ($V \cong$ 100–300 cm^3) filled with hyperpolarized ^{3}He gas. The irregular shape of cell wall in (b) is clearly depicted. Experimental parameters: (a) 2D FLASH, TR = 150 ms, TE = 5 ms, FOV = 180 × 180 mm^2, matrix 128 × 256, N = 1; (b) 2D FLASH, TR = 225 ms, TE = 5 ms, FOV = 230 × 230 mm^2, matrix 192 × 256, N = 1; (c, d) 3D FLASH, TR = 22 ms, TE = 6 ms, FOV = 250 × 250 mm^2, matrix 256 × 256, N = 1, 96 mm slab, and 32 partitions resulting in 3 mm slice thickness.

The comparison of proton (Fig. 3a) and ^{3}He images (Figs. 3b and 3c) demonstrates that ^{3}He MRI depicts anatomical structures reliably. The distribution of ^{3}He is visible in the nasal cavity and in the pharyngeal space. Images reflect the complex structure (#1 in Fig. 3c) and the dorsal boundary (#2) of the nasal conchae consistent with findings in conventional proton MR images. High ^{3}He MR signal intensity is seen at the caudal aspect of the nasal cavity (#3) and in the nasopharynx (#4). The dorsal displacement of the tongue at breath-hold produces a discontinuity of the ^{3}He column that results in missing signal in the oropharynx (#5). The strongest ^{3}He MR signal intensity is found in the hypopharynx (#6). The apparent bifurcation in the hypopharynx is caused by the arythenoideal muscle (#7).

In the second and third series, a strong decrease of ^{3}He signal intensity was detected (indicating, as expected, much faster T_1 relaxation of ^{3}He spins *in vivo* than in the glass cells), except for the hypopharynx (#6 in Fig. 3c). This region showed all the time sufficient signal intensity, the hypopharynx being blocked by the tongue at breath-hold to the upper hollow spaces like the nasal cavity (#3).

In Experiment 2 the volunteer's thorax was examined after deep inhalation of hyperpolarized ^{3}He gas, immediately after previous flushing with ^{4}He. Figures 4a and

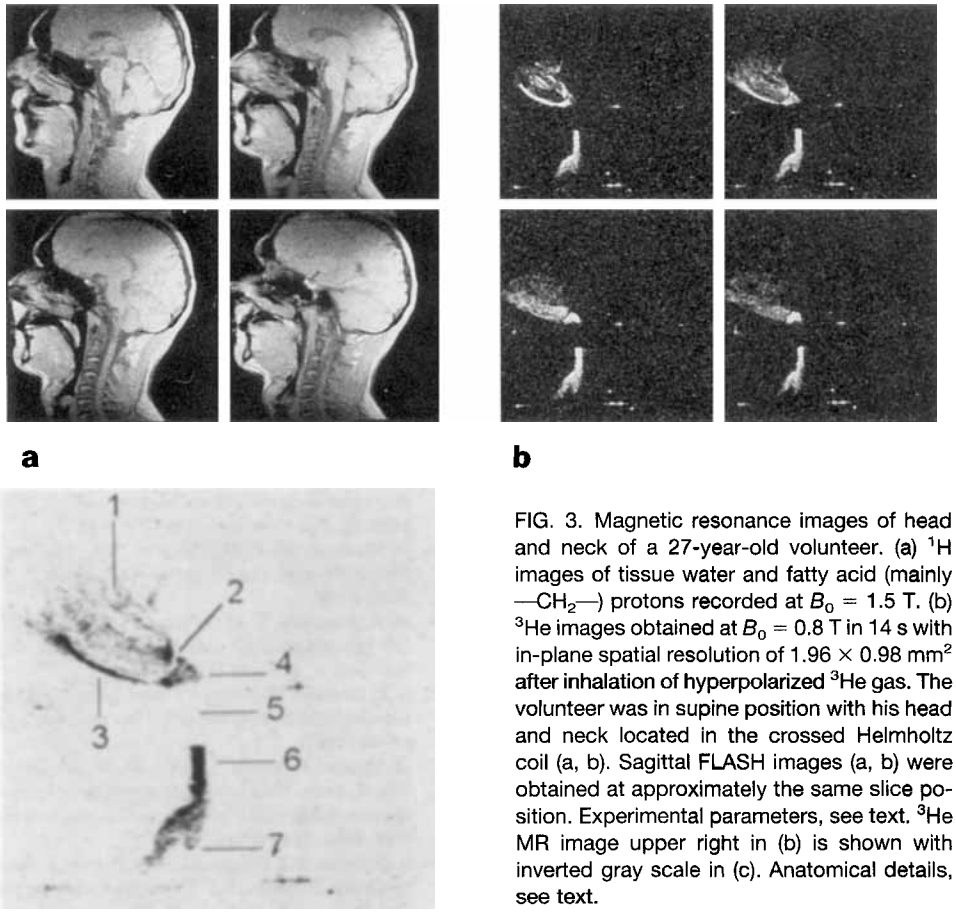

FIG. 3. Magnetic resonance images of head and neck of a 27-year-old volunteer. (a) ^1H images of tissue water and fatty acid (mainly —CH_2—) protons recorded at B_0 = 1.5 T. (b) ^3He images obtained at B_0 = 0.8 T in 14 s with in-plane spatial resolution of 1.96 × 0.98 mm^2 after inhalation of hyperpolarized ^3He gas. The volunteer was in supine position with his head and neck located in the crossed Helmholtz coil (a, b). Sagittal FLASH images (a, b) were obtained at approximately the same slice position. Experimental parameters, see text. ^3He MR image upper right in (b) is shown with inverted gray scale in (c). Anatomical details, see text.

4b show ^1H and ^3He FLASH images of the lungs of the volunteer. *In vivo* ^3He MR images were acquired with the same procedure as in Experiment 1, except the longer measurement time of 3 × 28 s (13). In the first two of the three series, a strong signal intensity in ventilated regions was observed (images in Fig. 4b were obtained during the first series). The distribution of hyperpolarized ^3He in the hollow organ is clearly depicted, with intense signal outlining the pulmonary airway and signal void in the vascular and cardiac structures. It agrees well with regions void of signal within the lung parenchyma and with regions of high signal from the vascular system in the corresponding sagittal ^1H FLASH images. A homogeneous distribution of ^3He gas in all lung segments is seen, and the ventilated air space is completely visualized. Some signal from within the trachea can be observed. Similar to scintigraphic images, the signal intensity drops off in the apical regions of the lungs. The signal seen outside of the thorax originates from residual ^3He gas within the glass cell placed on top of the volunteer's sternum.

The evaluation of the ^3He MR signal intensities of a selected region in the images of the first and second series of Experiment 2 yields the ratio $S_2/S_1 \cong 0.46$. Accordingly, the flip angle was $\leq 4°$ in this experiment (n = 256). On the other hand, when the depletion of polarization due to RF excitation is negligible, the relaxation time constant of ^3He *in vivo* can be estimated from this ratio. With a measurement time of 28 s in this experiment, we obtain $T_1 = -28$ s/ln 0.46 ≅ 36 s.

DISCUSSION

Spin imaging of inhaled hyperpolarized ^3He gas allows the visualization of air-filled spaces in the human body. In particular, ventilated regions of the lungs can be mapped by means of this technique.

Several series of multislice imaging with spatial resolution comparable with that of proton MRI were possible, because of sufficiently long half-life of the enhanced spin polarization in the airways. The experiment was performed in a conventional whole-body MR tomograph and establishes a new diagnostic imaging technique without ionizing radiation of the human respiratory system.

Hyperpolarized nuclei in the gas phase yield very high MR signals *in vivo* that allow the study of ventilation in lungs systematically with fast magnetic resonance imaging. Monitoring of ventilation by means of this technique could be an alternative to established nuclear medicine methods. To facilitate clinical application of ^3He MRI of the thorax, an appropriate volume resonator is required, which also allows simultaneous proton MR imaging.

^3He MRI is an interesting alternative to ^{129}Xe imaging (14), because of the larger magnetic moment of the nucleus and higher achievable spin polarization. Moreover,

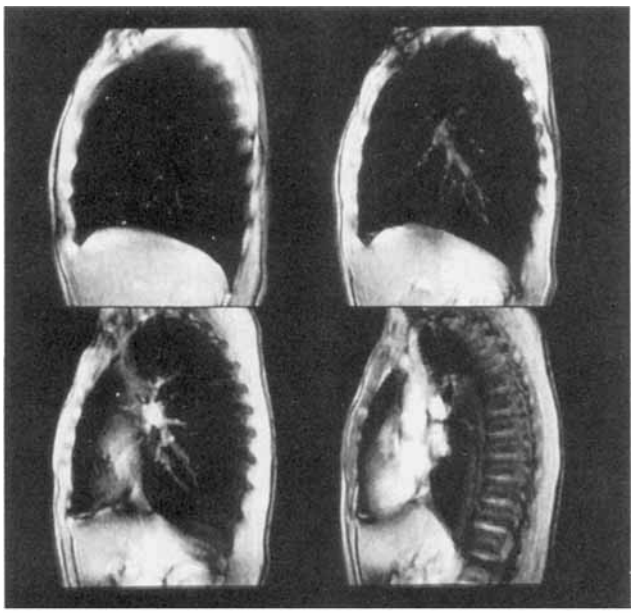

a

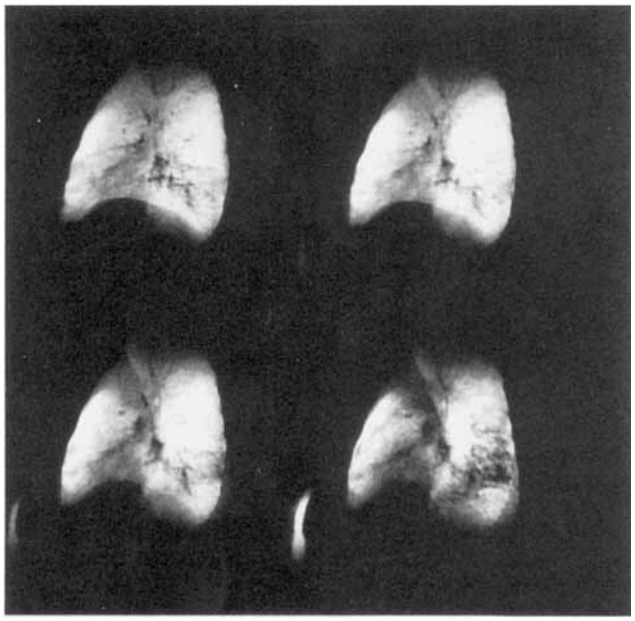

b

FIG. 4. Magnetic resonance images of the lungs (volunteer in Fig. 2). (a) ^{1}H images recorded at $B_0 = 1.5$ T. (b) ^{3}He images obtained at $B_0 = 0.8$ T in 28 s with in-plane spatial resolution of 1.17×1.17 mm^2 immediately after inhalation of hyperpolarized ^{3}He gas. Sagittal FLASH images were obtained with the body resonator (a) and with the Helmholtz coil (b) at approximately the same slice position. Experimental parameters, see text.

^{3}He should be inert in contrast to ^{129}Xe, which is a general anesthetic, and hence should not induce adverse effects on single inhalation. A disadvantage is the high cost of the rare isotope ^{3}He, which demands recovery. An integrated device for production, storage, and delivery of hyperpolarized ^{3}He is now under construction.

ACKNOWLEDGMENTS

The authors thank Professor Dr. W. J. Lorenz, Professor Dr. G. van Kaick, Professor Dr. M. Thelen, and Dr. M. Leduc for their support; and H. Groβ and F.-P. Boroch, Siemens Medical Systems, for technical assistance.

REFERENCES

1. C. J. Bergin, J. M. Pauly, A. Macovski, Lung parenchyma: projection reconstruction MR imaging. *Radiology* **179,** 777–781 (1991).
2. A. A. Maudsley, S. K. Hilal, H. E. Simon, S. Wittekoek, *In vivo* spectroscopic imaging with ^{31}P. *Radiology* **153,** 745–750 (1984).
3. C. W. Li, W. Negendank, P. O'Dwyer, K. Padavic-Shaller, J. Murphy-Boesch, T. R. Brown, MRI-directed, 3D-CSI-localized ^{19}F MRS of fluorouracil catabolism in human liver, *in* "Proc., SMR, 2nd Annual Meeting, San Francisco, 1994," p. 1303.
4. D. Neuhaus, M. P. Williamson, "The Nuclear Overhauser Effect in Structural and Conformational Analysis," VCH Publishers, New York, 1989.
5. M. A. Bouchiat, T. R. Carver, C. M. Varnum, Nuclear polarization in ^{3}He gas induced by optical pumping and dipolar exchange. *Phys. Rev. Lett.* **5,** 373–375 (1960).
6. N. D. Bhaskar, W. Happer, T. McClelland, Efficiency of spin exchange between rubidium spins and ^{129}Xe nuclei in a gas. *Phys. Rev. Lett.* **49,** 25–28 (1982).
7. W. Happer, E. Miron, S. Schaefer, D. Schreiber, W. A. van Wijngaarden, X. Zeng, Polarization of the nuclear spins of noble-gas atoms by spin exchange with optically pumped alkali-metal atoms. *Phys. Rev.* **A29,** 3092–3110 (1984).
8. G. D. Cates, R. J. Fitzgerald, A. S. Barton, P. Bogorad, M. Gatzke, N. R. Newbury, B. Saam, Rb-^{129}Xe spin-exchange rates due to binary and three-body collisions at high Xe pressures. *Phys. Rev.* **A45,** 4631–4639 (1992).
9. F. D. Colegrove, L. D. Schearer, G. K. Walters, Polarization of ^{3}He gas by optical pumping. *Phys. Rev.* **132,** 2561–2572 (1963).
10. G. Eckert, W. Heil, M. Meyerhoff, E. W. Otten, R. Surkau, M. Werner, M. Leduc, P. J. Nacher, L. D. Schearer, A dense polarized ^{3}He target based on compression of optically pumped gas. *Nucl. Instrum. Meth.* **A320,** 53–65 (1992).
11. J. Becker, W. Heil, B. Krug, M. Leduc, M. Meyerhoff, P. J. Nacher, E. W. Otten, T. Prokscha, L. D. Schearer, R. Surkau, Study of mechanical compression of spin-polarized ^{3}He gas. *Nucl. Instrum. Methods* **A346,** 45–51 (1994).
12. W. Heil, H. Humblot, E. W. Otten, M. Schafer, R. Surkau, M. Leduc, Very long nuclear relaxation times of spin polarized helium 3 in metal coated cells. *Phys. Lett.* **A201,** 337–343 (1995).
13. M. Ebert, T. Großmann, W. Heil, E. W. Otten, R. Surkau, M. Leduc, P. Bachert, M. V. Knopp, L. R. Schad, M. Thelen, Nuclear magnetic resonance imaging with hyperpolarised helium-3. *Lancet* **347,** 1297–1299 (1996).
14. M.S. Albert, G.D. Cates, B. Drlehuys, W. Happer, B. Saam, C.S. Springer, A. Wishnia, Biological magnetic resonance imaging using laser-polarized ^{129}Xe. *Nature* **370,** 199–200 (1994).
15. H. Middleton, R. D. Black, B. Saam, G. D. Cates, G. P. Cofer, R. Guenther, W. Happer, L. W. Hedlund, G. A. Johnson, K. Juvan, J. Swartz, MR imaging with hyperpolarized ^{3}He gas. *Magn. Reson. Med.* **33,** 271–275 (1995).
16. L. D. Schearer, G. K. Walters, Nuclear spin-lattice relaxation in the presence of magnetic-field gradients. *Phys. Rev.* **139,** A1398–A1402 (1965).
17. A. Haase, J. Frahm, D. Matthaei, W. Hänicke, K.-D. Merboldt, FLASH imaging. Rapid NMR imaging using low flip-angle pulses. *J. Magn. Reson.* **67,** 258–266 (1986).
18. B. Saam, W. Happer, H. Middleton, Nuclear relaxation of ^{3}He in the presence of O_2. *Phys. Rev.* **A52,** 862–865 (1995).